SUPERSONIC TURBULENT BOUNDARY LAYER ON A PLATE. ASYMPTOTIC STRUCTURE AND SIMILARITY LAWS

Igor Vigdorovich
Institute of Mechanics
Lomonosov Moscow State Univesity
Michurinsky ave. 1, 119192 Moscow, Russia
vigdorovich@imec.msu.ru

ABSTRACT

An asymptotic theory of a turbulent boundary layer on a flat plate at moderate supersonic free-stream Mach numbers is developed. Its main elements are: the formulation of simple exact closure relations for the Reynolds and energy equations and a procedure for solving these equations by the method of matched asymptotic expansions at large Reynolds numbers. As a result, a complete description of the flow is given in terms of similarity laws for the main dynamic and thermal quantities, which are valid in the viscous, logarithmic and outer regions of the boundary layer. The Crocco integral, which relates the velocity and temperature profiles in the logarithmic region, and the laws of the wall for velocity and temperature are obtained. For any wall-heat-transfer conditions, velocity and temperature defect laws have been established, which make it possible to describe the profiles of these quantities in the outer and logarithmic regions by universal curves known for the boundary layer of an incompressible fluid. The recovery and Reynolds-analogy factors are calculated. A friction law is established that is valid under arbitrary wall-heat-transfer conditions.

PROBLEM FORMULATION AND CLOSURE RELATIONS

We consider a compressible turbulent boundary layer on a flat plate in a uniform stationary stream with velocity u_∞, density ρ_∞, viscosity μ_∞, and enthalpy h_∞. The gas enthalpy at the plate h_w is constant. The gas is perfect with heat capacity ratio γ. The coefficients of viscosity μ and thermal conductivity k are power functions of temperature with the exponent n, while the molecular Prandtl number $Pr = c_p\mu/k$ is a constant quantity.

The flow is described by the compressible turbulent boundary-layer equations

$$\overline{\rho}\tilde{u}\frac{\partial \tilde{u}}{\partial x} + \overline{\rho}\tilde{v}\frac{\partial \tilde{u}}{\partial y} = \frac{\partial}{\partial y}\left(\overline{\mu\frac{\partial u}{\partial y}} - \overline{\rho}\,\widetilde{u''v''}\right),$$

$$\frac{\partial \overline{\rho}\tilde{u}}{\partial x} + \frac{\partial \overline{\rho}\tilde{v}}{\partial y} = 0,$$

$$\overline{\rho}\tilde{u}\frac{\partial \tilde{h}}{\partial x} + \overline{\rho}\tilde{v}\frac{\partial \tilde{h}}{\partial y} = \frac{\partial}{\partial y}\left[\overline{\frac{k}{c_p}\frac{\partial h}{\partial y}} + \overline{\mu u\frac{\partial u}{\partial y}} - \overline{\rho}\widetilde{h''v''}\right.$$

$$\left. -\frac{\overline{\rho}}{2}(\widetilde{u''^2v''} + \widetilde{v''^3} + \widetilde{v''w''^2})\right] - \tilde{u}\frac{\partial}{\partial y}\left(\overline{\mu\frac{\partial u}{\partial y}}\right) - \overline{\rho}\frac{\partial \tilde{u}}{\partial y}\widetilde{u''v''},$$

$$\overline{\rho}\,\tilde{h} = \frac{\gamma p_\infty}{(\gamma-1)}. \tag{1}$$

Here, we use Favre's averaging with density as a weighting function.

The description of turbulent flows in the framework of the averaged Navier–Stokes equations always faces a fundamental problem of finding additional relations to close the problem. Modern theory of turbulence models is known to be devoted to a practical solution to this problem. However, due to a semi-empirical nature of the theory, its results are non-rigorous and approximate. We propose another approach to the closure problem, which can be applied to a relatively narrow class of canonical flows, but is free from partial hypotheses and is based only on first principles. According to the idea first put forward by Vigdorovich (2003), if the flow as a whole depends on a finite number of constant parameters, the turbulent shear stress and turbulent heat flux can be represented as functions of the mean longitudinal-velocity and temperature gradients. For the supersonic turbulent boundary layer on a plate, the type of such functional relations is established by Vigdorovich (2023a), and they have the form

$$\widetilde{u''v''} = -\left(y\frac{\partial \tilde{u}}{\partial y}\right)^2 S(\mathrm{Re}, \mathrm{Pe}, n, \eta, \Pi_1, \Pi_2, \Gamma), \tag{2}$$

$$\widetilde{h''v''} + \tfrac{1}{2}\left(\widetilde{u''^2v''} + \widetilde{v''^3} + \widetilde{v''w''^2}\right)$$

$$= -y^2\frac{\partial \tilde{h}}{\partial y}\frac{\partial \tilde{u}}{\partial y}H(\mathrm{Re}, \mathrm{Pe}, n, \eta, \Pi_1, \Pi_2, \Gamma), \tag{3}$$

$$\widetilde{h''^2} = \left(y\frac{\partial \tilde{h}}{\partial y}\right)^2 G(\mathrm{Re}, \mathrm{Pe}, n, \eta, \Pi_1, \Pi_2, \Gamma), \tag{4}$$

$$\mathrm{Re} = \frac{\overline{\rho}y^2}{\tilde{\mu}}\frac{\partial \tilde{u}}{\partial y}, \quad \mathrm{Pe} = Pr\mathrm{Re}, \quad \eta = \frac{y}{\delta},$$

$$\Pi_1 = \frac{y(\partial\tilde{u}/\partial y)^2}{\partial\tilde{h}/\partial y}, \quad \Pi_2 = \frac{y}{\tilde{h}}\frac{\partial \tilde{h}}{\partial y}, \quad \Gamma = \frac{\gamma\Pi_1\Pi_2}{\gamma-1},$$

where δ is the boundary-layer thickness. The universal functions S, H and G have the asymptotic expansions

$$S = S_0(\mathrm{Re}, \eta) + \Pi_2 S_2(\mathrm{Re}, \mathrm{Pe}, n/\mathrm{Re}, \eta) + O(\Pi_1\Pi_2) + O(\Pi_2^2), \tag{5}$$

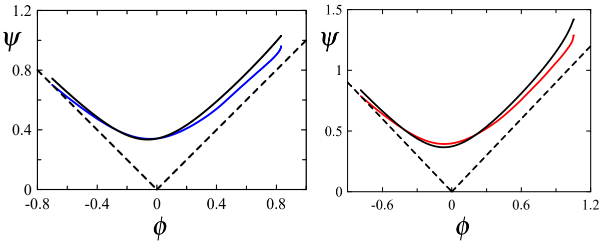

Figure 1. Temperature-velocity dependence in variables $(\phi,\, \psi)$. The blue and red curves correspond to the DNS data (Zhang et al., 2018) at $Q_+ = -0.14$ $(h_w/h_r = 0.25)$, $M_\infty = 5.84$ and $Re_\tau = 450$ and $Q_+ = -0.19$ $(h_w/h_r = 0.18)$, $M_\infty = 13.64$ and $Re_\tau = 646$, respectively; the black curves correspond to formula (9); the dashed lines correspond to the Walz (1966) equation.

$$H = H_0(\mathrm{Re}, \mathrm{Pe}, \eta) + \Pi_1 H_1(\mathrm{Re}, \mathrm{Pe}, \eta) + \Pi_2 H_2(\mathrm{Re}, \mathrm{Pe}, n/\mathrm{Re}, \eta)$$

$$+O(\Pi_1\Pi_2) + O(\Pi_2^2), \tag{6}$$

$$G = G_0(\mathrm{Re}, \mathrm{Pe}, \eta) + \Pi_1 G_1(\mathrm{Re}, \mathrm{Pe}, \eta) + \Pi_1^2 G_2(\mathrm{Re}, \mathrm{Pe}, \eta)$$

$$+\Pi_2 G_3(\mathrm{Re}, \mathrm{Pe}, n/\mathrm{Re}, \eta) + O(\Pi_1\Pi_2) + O(\Pi_2^2), \quad \Pi_2 \to 0. \tag{7}$$

Since the parameter Π_2 expresses the relative enthalpy drop across the boundary layer and thus characterises flow compressibility, the first terms in expansions (5)–(7), the functions S_0, H_0 and G_0, correspond to incompressible flow.

In what follows, we will use the abbreviated notations

$$\begin{aligned} &S\,(\infty, \infty, n, \eta, \Pi_1, \Pi_2, \Gamma) = S_e\,(\eta, \Pi_1, \Pi_2, \Gamma)\,, \\ &H\,(\infty, \infty, n, \eta, \Pi_1, \Pi_2, \Gamma) = H_e\,(\eta, \Pi_1, \Pi_2, \Gamma)\,, \end{aligned} \tag{8}$$

which take into account that at $\mathrm{Re} \to \infty$, the molecular viscosity and thermal conductivity and hence the value of n, which specifies the viscosity law, are not significant outside the viscous sublayer.

VISCOUS AND LOGARITHMIC SULAYERS

We distinguish three characteristic regions in the boundary layer: a viscous sublayer near the wall, where turbulent and viscous stresses as well as turbulent and molecular heat transfer are of the same order of magnitude; an outer region, which is also called the wake region or the region of a velocity-defect law, where molecular viscosity and thermal conductivity can be neglected; and an inertial or logarithmic sublayer located between them. The latter is characterized by the fact that both inertial and viscous terms in the momentum and energy equations can be neglected in it.

In the viscous and logarithmic sublayers, the solution is constructed in the form of expansions in the small parameter $\varepsilon = u_\tau/\sqrt{2h_w}$ that is proportional to the Mach number formed with the friction velocity u_τ and the speed of sound at the wall. Three characteristic flow regimes are possible in the viscous sublayer, which occur at small (including zero), moderate (positive or negative), and large negative wall heat flux. For the first two regimes, the flow in the viscous sublayer is incompressible to a first approximation, the dimensionless velocity profile is the same as in an incompressible fluid (Vigdorovich, 2017, 2023b), while the temperature profile is a superposition of the temperature profile in the incompressible boundary layer and the boundary layer on an adiabatic wall (Vigdorovich, 2023b). In the viscous sublayer on a strongly cooled plate, compressibility is significant. The case of a heated plate always refers to the moderate heat-flux regime.

The Crocco integral in the logarithmic region and the laws of the wall for velocity and temperature read

$$\cos^2\psi = \cos^2\phi - \varepsilon_* P(\phi,\, \phi_w) + O(\varepsilon^2), \quad \phi_w \le \phi < \frac{\pi}{2}, \tag{9}$$

$$\frac{\phi - \phi_w}{\varepsilon_*} + Q_1(\phi,\, \phi_w) + O(\varepsilon) = \frac{1}{\kappa}\ln y_+ + D_1(Pr,\, n,\, Q_+) + O(y_+^{-\alpha}), \tag{10}$$

$$\frac{\psi - \phi_w}{\varepsilon_*} + R(\psi,\, \phi_w) + O(\varepsilon) = \frac{1}{\kappa}\ln y_+ + D_1(Pr,\, n,\, Q_+) + O(y_+^{-\alpha}),$$

$$\varepsilon_* = \sqrt{\sigma}\,\varepsilon, \quad y_+ \to \infty, \qquad \alpha > 0, \tag{11}$$

$$P(\phi,\, \phi_w) = 2A_1(\phi - \phi_w) + A_2\sin 2\phi + [D(Pr) - C - A_2]\sin 2\phi_w,$$

$$Q_1(\phi,\, \phi_w) = A_1(\phi - \phi_w)\tan\phi + A_3\ln\frac{\cos\phi}{\cos\phi_w}$$

$$-A_2\frac{\sin\phi_w\sin(\phi - \phi_w)}{\cos\phi} + [D(Pr) - C]\frac{\cos\phi_w\cos(\phi - \phi_w)}{\cos\phi},$$

$$R(\psi,\, \phi_w) = -A_1(\psi - \phi_w)\cot\psi + A_3\ln\frac{\cos\psi}{\cos\phi_w}$$

$$+[D(Pr) - C - A_2]\frac{\cos\phi_w\sin(\psi - \phi_w)}{\sin\psi}.$$

These relationships are written in similarity variables, which are specified by the equalities

$$\sin\phi = \frac{\sqrt{\sigma}(\tilde{u} + q_w/\tau_w)}{\sqrt{2h_w + \sigma(q_w/\tau_w)^2}}, \quad \cos\psi = \frac{\sqrt{2\tilde{h}}}{\sqrt{2h_w + \sigma(q_w/\tau_w)^2}}.$$

Here, τ_w and q_w are the shear stress and heat flux on the wall, respectively, while ϕ_w is the value of the variable ϕ at $\tilde{u} = 0$. In addition to the von Kármán constant $\kappa = 0.41$, turbulent Prandtl number in the logarithmic region $\sigma = 0.85$ and quantities $C = 5.2$ and $D(0.72) = 4.6$, which are included in the logarithmic laws for velocity and temperature in the incompressible boundary layer (Vigdorovich, 2017, 2023b), relations (9)–(11) contain three new universal constants $A_1 = 0.29$, $A_2 = 0.59$ and $A_3 = 1.95$ determined in (Vigdorovich, 2023b, 2024) by comparison with DNS data. The empirical function $D_1(Pr, n, Q_+)$ depends on the molecular Prandtl number, the law of viscosity and heat conductivity, which in this case is specified by the exponent n, and the dimensionless heat flux $Q_+ = q_w/h_w\sqrt{\rho_w\tau_w}$. The equality $D_1(Pr, n, 0) = D(Pr)$ holds.

In the zero-order approximation for the small parameter, the Crocco integral (9) is the Waltz equation (Walz, 1966), but unlike it, it describes well the relationship between velocity and temperature in the boundary layer on a cooled wall. This can be seen in figure 1, where formula (9) is compared with the DNS data (Zhang et al., 2018) for the boundary layer on a strongly cooled plate.

The law of the wall for velocity is given by relation (10), on the left-hand side of which is an asymptotic expansion in

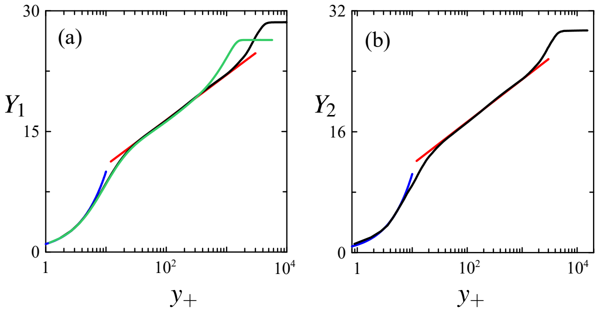

Figure 2. DNS data for the velocity and temperature profiles in the supersonic boundary layer on an adiabatic wall at $M_\infty = 2$ and $Re_\tau = 4000$ (Pirozzoli & Bernardini, 2013) (black curves) and $M_\infty = 2$ and $Re_\tau = 1468$ (Appelbaum et al., 2025) (green curve) plotted in similarity variables (12) and (13); Y_1 and Y_2 are the left-hand sides of equations (12) and (13), respectively. In panels (a) and (b) the red lines correspond to the logarithmic laws $\kappa^{-1}\ln y_+ + C$ and $\kappa^{-1}\ln y_+ + C + A_1 + A_2$, respectively, and the blue curves specify the linear and parabolic profiles, respectively.

the parameter ε, whose leading term coincides with the Van Driest (1951) formula. The difference from the Van Drist formula is provided by the second term of the expansion (the function Q_1), which is of order one.

In the case of an adiabatic plate, the laws of the wall for velocity and temperature can be written as (Vigdorovich, 2024)

$$\frac{\phi}{\varepsilon_*} + A_3 \ln\cos\phi + A_1\phi\tan\phi + O(\varepsilon) = U_+(y_+), \tag{12}$$

$$\frac{\psi}{\varepsilon_*} + A_1(1-\psi\cot\psi) + A_3\ln\cos\psi + O(\varepsilon) = \sqrt{\frac{2T_+^0(y_+)}{\sigma}}, \tag{13}$$

$$\phi = \arcsin\sqrt{\frac{\sigma\tilde{u}^2}{2h_r}},\quad \psi = \arccos\sqrt{\frac{\tilde{h}}{h_r}},\quad \varepsilon_* = \sqrt{\frac{\sigma u_\tau^2}{2h_r}},\quad y_+ \ge 0,$$

where $U_+(y_+)$ is the known velocity profile in the near-wall region of the incompressible boundary layer, and $T_+^0(y_+)$ is the temperature profile in the near-wall region of the incompressible boundary layer on an adiabatic wall, investigated by Vigdorovich (2024). The latter has the following asymptotic behaviour on the wall and in the logarithmic sublayer:

$$T_+^0 = \frac{1}{2}(Pr+b)y_+^2 + O(y_+^3),\quad y_+ \to 0, \tag{14}$$

$$\sqrt{\frac{2T_+^0}{\sigma}} = \frac{1}{\kappa}\ln y_+ + C + A_1 + A_2 + O\left(\ln^{-1} y_+\right),\quad y_+ \to \infty, \tag{15}$$

where b is obtained from the following relation for the incompressible boundary layer:

$$\overline{u_+'^2} = by_+^2 + O(y_+^3),\quad y_+ \to 0,\quad b \approx 0.17.$$

The relations (12)–(15) are fully confirmed by the DNS data presented in figure 2.

Consider now root-mean-square enthalpy fluctuations. Figure 3(a) shows the profiles of this quantity together with the enthalpy profiles in the boundary layer on a cooled wall

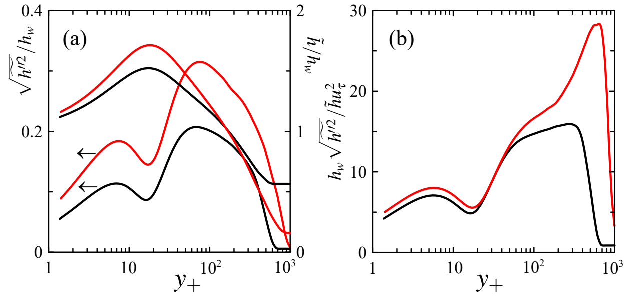

Figure 3. Enthalpy and root-mean-square enthalpy fluctuations [panel (a)] and transformed root-mean-square enthalpy fluctuations [panel (b)] in the boundary layer on a cooled plate according to the DNS data by Zhang et al. (2018) at $M_\infty = 5.84$, $Re_\tau = 450$ and $Q_+ = -0.14$ (black curves) and $M_\infty = 13.64$, $Re_\tau = 646$ and $Q_+ = -0.19$ (red curves).

(Zhang et al., 2018). As can be seen in figure 3(a), the root-mean-square enthalpy fluctuation in the logarithmic region has a dip and a local minimum located approximately at the enthalpy maximum point. Using (4) and the quadratic dependence (7) of the asymptotics of the function G on the variable Π_2, Vigdorovich (2024) explained this behavior and obtained the representation of the enthalpy fluctuation in the vicinity of the minimum point

$$\frac{h_w\sqrt{\widetilde{h''^2}}}{\tilde{h}u_\tau^2} = \frac{1}{\kappa^2}\sqrt{G_2(\infty,\infty,0)} + O(\varepsilon),$$

which gives a similarity rule for this quantity. Figure 3(b) shows that this similarity rule really allows one to match the minimum points on the root-mean-square enthalpy-fluctuation profiles obtained at different Mach numbers and wall heat-flux values.

OUTER REGION OF THE BOUNDARY LAYER

We consider the outer region of the boundary layer at moderate supersonic free-stream Mach numbers, when the relative temperature difference across the layer is of order one.

After introducing the stream function $\psi_y = \overline{\rho}\tilde{u}$ and $\psi_x = -\overline{\rho}\tilde{v}$ and new variables by formulas (Vigdorovich, 1993, 2025)

$$\psi = \rho_\infty u_\infty \delta \Psi(\xi,\eta),\quad \tilde{h} = h_\infty + u_\infty^2\Phi(\xi,\eta),\quad \overline{\rho} = \rho_\infty\omega(\xi,\eta),$$

$$\xi = \ln Re_\delta,\quad Re_\delta = \frac{\sqrt{\rho_\infty\rho_w}\,u_\infty\delta}{\mu_w}, \tag{16}$$

we obtain from the boundary-layer equations (1) as well as closure relations (2) and (3) the following equations:

$$\Lambda\left[\Psi_\eta(\omega^{-1}\Psi_\eta)_\xi - (\Psi+\Psi_\xi)(\omega^{-1}\Psi_\eta)_\eta\right] = \left\{\omega\left[\eta(\omega^{-1}\Psi_\eta)_\eta\right]^2 S_e(\eta,\Pi_1,\Pi_2,\Gamma)\right\}_\eta, \tag{17}$$

$$\Lambda[\Psi_\eta\Phi_\xi - (\Psi+\Psi_\xi)\Phi_\eta] = \left[\omega\eta^2\Phi_\eta(\omega^{-1}\Psi_\eta)_\eta H_e(\eta,\Pi_1,\Pi_2,\Gamma)\right]_\eta + \omega\eta^2\left[(\omega^{-1}\Psi_\eta)_\eta\right]^3 S_e(\eta,\Pi_1,\Pi_2,\Gamma), \tag{18}$$

$$\Lambda(\xi) = \frac{\mathrm{d}\delta}{\mathrm{d}x}, \ \ \omega^{-1} = 1 + (\gamma - 1)M_\infty^2 \Phi, \tag{19}$$

$$\Pi_1 = \frac{\eta[(\omega^{-1}\Psi_\eta)_\eta]^2}{\Phi_\eta}, \ \ \Pi_2 = -\frac{\partial \ln \omega}{\partial \ln \eta},$$

which use the logarithm of the Reynolds number based on the boundary-layer thickness ξ and the normalized distance from the wall η as independent variables. In addition to the dimensionless stream function $\Psi(\xi,\eta)$ and enthalpy $\Phi(\xi,\eta)$, the third unknown function $\Lambda(\xi)$, the growth rate of the boundary-layer thickness, is introduced. Since equations (17) and (18) are used only in the outer region of the boundary layer, the molecular viscosity and thermal conductivity terms are omitted, and the local Reynolds and Peclet numbers are set equal to infinity, which allows the notation (8) to be used.

Equations (17) and (18) are convenient for asymptotic analysis, since the boundary-layer thickness growth rate Λ is a small quantity and the variable ξ equal to the logarithm of Reynolds number is a large quantity, which makes it possible to search for an asymptotic solution of the problem as $\xi \to \infty$. The change of variables (16) and the equations for the desired functions (17) and (18) were first proposed by Vigdorovich (1993) for the boundary layer of an incompressible fluid.

In the outer region of the boundary layer that is characterised by the condition $1/\eta = O(1)$, we look for the solution of equations (17) and (18) in the form (Vigdorovich, 2017, 2025)

$$\Lambda = \lambda_1\zeta^{-1} + O(\zeta^{-2}), \ \ \frac{\tilde{u}}{u_\infty} = \frac{\Psi_\eta}{\omega} = 1 + \lambda_1 f_0(\eta)\zeta^{-1} + O(\zeta^{-2}),$$

$$\Phi = \lambda_2\varphi_0(\eta)\zeta^{-1} + O(\zeta^{-2}), \ \ \xi = \zeta + k\ln\zeta, \ \ \zeta \to \infty, \tag{20}$$

where the constant coefficients λ_1, λ_2 and k are to be determined. For the dimensionless density, equalities (19) and (20) give

$$\omega^{-1} = 1 + (\gamma - 1)M_\infty^2 \lambda_2 \varphi_0(\eta)\zeta^{-1} + O(\zeta^{-2}), \tag{21}$$

which shows that at moderate free-stream Mach numbers $M_\infty = O(1)$, the flow in the outer region is, to a first approximation, incompressible.

By substituting the expansions (20) and (21) into equations (17) and (18) and taking the limit as $\zeta \to \infty$ with $1/\eta = O(1)$, we obtain in view of the asymptotic expansions (5) and (6) the ordinary differential equations for the functions f_0 and φ_0

$$\left[(\eta f_0')^2 S_0(\infty,\eta)\right]' + \eta f_0' = 0; \quad f_0(\infty) = 0, \tag{22}$$

$$\left[\eta^2 \varphi_0' f_0' H_0(\infty,\infty,\eta)\right]' + \eta\varphi_0' = 0; \quad \varphi_0(\infty) = 0. \tag{23}$$

The last term in equation (18) related to kinetic heating has a higher order of smallness and is not included in equation (23).

Equations (22) and (23) coincide completely with those obtained by Vigdorovich (2017) for the incompressible boundary layer.

As a result of the asymptotic matching of the solutions for the outer region and logarithmic sublayer, the velocity and temperature defect laws are obtained (Vigdorovich, 2025)

$$\frac{\phi_\infty - \phi}{\tan\vartheta\sqrt{\frac{1}{2}C_f}} = f_0(\eta)\left[1 + O\left(\sqrt{C_f}\right)\right], \tag{24}$$

$$\frac{\psi_\infty - \psi}{\tan\vartheta\sqrt{\frac{1}{2}C_f}} = \varphi_0(\eta)\left[1 + O\left(\sqrt{C_f}\right)\right], \tag{25}$$

$$\tan\vartheta = M_\infty\sqrt{\frac{\sigma}{2}(\gamma - 1)}.$$

Here, $\phi_\infty = \phi(u_\infty)$ and $\psi_\infty = \psi(h_\infty)$ are the values of the variables ϕ and ψ at the outer edge of the boundary layer, the functions $f_0(\eta)$ and $\varphi_0(\eta)$ are the same as in the incompressible boundary layer (Vigdorovich, 2017). The velocity-defect law (24) is valid in the outer and logarithmic regions of the boundary layer, i.e. everywhere outside the viscous sublayer. The same applies to the temperature-defect law (25) for a non-negative wall heat flux. In the case of a cooled plate, the temperature changes non-monotonically across the layer, and relation (25) is valid above the point of maximum temperature. Relations (24) and (25) are well confirmed by the available calculated and experimental data for all wall-heat-transfer conditions at free-stream Mach numbers less than three. In figure 4, the DNS data for the boundary layer on an adiabatic plate are plotted in the similarity variables (24) and (25). The thickness of the boundary layer δ is expressed as $\delta_u\sqrt{2/C_f}$ and $\delta_h\sqrt{2/C_f}$, where δ_u and δ_h are the velocity and enthalpy defect thicknesses, respectively,

$$\delta_u = \int_0^\infty \left(1 - \frac{\tilde{u}}{u_\infty}\right)\mathrm{d}y, \quad \delta_h = \frac{\int_0^\infty (\tilde{h} - h_\infty)\mathrm{d}y}{h_w - h_\infty + \frac{1}{2}\sigma u_\infty^2}.$$

These quantities specify characteristic transverse scales of the dynamic and thermal boundary layers. The quantity $\delta_u\sqrt{2/C_f}$ is similar to the Clauser-Rotta boundary-layer thickness known for an incompressible fluid. In figure 4(*a*), the calculated velocity profiles in the incompressible (curve 2) (Schlatter & Örlü, 2010) and compressible supersonic boundary layer at $M_\infty = 2$ (curves 3–5) (Pirozzoli & Bernardini, 2011, 2013), outside the viscous sublayer, practically, describe a single curve, which can also be specified by the Coles formula for an incompressible fluid (curve 1) (Vigdorovich, 2017), while the Reynolds number affects only the logarithmic-section extent. The temperature profiles obtained at $M_\infty = 2$ (figure 4*b*) behave in the same way; in the outer region and logarithmic sublayer, they are very close to the empirical approximation of the temperature profile for the incompressible boundary layer (curve 6) (Vigdorovich, 2017). Complete universality in Mach and Reynolds numbers is demonstrated by the experimental data (Fernholz & Finley, 1977, CAT 7302) in figures 4(*c,d*), where all experimental points obtained at Mach numbers from 0.8 to 2.8 and different Reynolds numbers, outside the viscous sublayer lie on the calculated curves corresponding to $M_\infty = 2$.

RECOVERY AND REYNOLDS-ANALOGY FACTORS

Another result of the asymptotic matching of the solutions for the outer region and the logarithmic sublayer are representations for the recovery and Reynolds-analogy factors r and $\alpha = 2St/C_f$ introduced by the formulas

$$h_r = h_\infty + \tfrac{1}{2}ru_\infty^2, \ \ St = \frac{q_w}{\rho_\infty u_\infty(h_w - h_r)},$$

where h_r is the recovery enthalpy and St is the Stanton number. The formulas have the form (Vigdorovich, 2025)

$$\frac{r}{\sigma} = 1 + \sqrt{2C_f}\left(\frac{A_0 - E_0}{\kappa} + A_2 + \frac{2A_1\vartheta}{\sin 2\vartheta}\right) + O(C_f), \quad (26)$$

$$\sigma\alpha = 1 + \sqrt{\tfrac{1}{2}C_f}\left[\frac{E_0 - A_0}{\kappa} - A_2 + [C + A_2 - D(Pr)]\sqrt{\frac{h_w}{h_\infty}}\right.$$

$$\left. + A_1 \cot\phi_w'\left(\frac{\vartheta}{\cos^2\vartheta} - \frac{\psi_\infty' - \phi_w'}{\cos^2\psi_\infty'}\right)\sqrt{\frac{h_\infty}{h_w}}\right] + O(C_f), \quad (27)$$

$$\psi_\infty' = \arctan\left[\frac{(2+\sigma Ec)\tan\vartheta}{2\sigma Ec}\right],$$

$$\phi_w' = \arctan\left[\frac{(2-\sigma Ec)\tan\vartheta}{2\sigma Ec}\sqrt{\frac{h_\infty}{h_w}}\right], \quad Ec = \frac{u_\infty^2}{h_w - h_\infty},$$

where Ec is the Eckert number characterising gas kinetic heating. Thus, just like Van Driest (1956), we have obtained the recovery factor (26) in the form of an asymptotic expansion in the small parameter — the root of the skin-friction coefficient. The leading term of the expansion is the turbulent Prandtl number in the logarithmic region σ, and the coefficient of the small parameter is a function of the Mach number and heat capacity ratio. In addition, relation (26) contains five more universal constants, three of which κ, $A_0 = 0.23$ and $E_0 = A_0 + \ln\sigma$ are known for the incompressible boundary layer (Vigdorovich, 2017), while A_1 and A_2 enter the Crocco integral for a compressible gas (9). Note that according to (26), the recovery factor with the accuracy of $O(C_f)$ is independent of the molecular Prandtl number. And this conclusion is supported by the expressions obtained by Van Driest (1956).

Formula (27) specifies the Reynolds-analogy factor in the form of an asymptotic expansion in the small parameter $\sqrt{C_f}$, the leading term of which is the reciprocal of the turbulent Prandtl number, which coincides in structure with the expression obtained by Van Driest (1956). Compared to the recovery factor, the number of parameters on which the Reynolds-analogy factor depends is two more due to the enthalpy ratio h_w/h_∞ and the molecular Prandtl number. The latter quantity enters (27) via the function $D(Pr)$, which is known from the logarithmic law for temperature in an incompressible fluid (Vigdorovich, 2017, 2023b). Equality (27) also includes the constant C from the logarithmic law for the velocity profile in an incompressible fluid (Vigdorovich, 2017, 2023b).

Formulas (26) and (27) allow us to calculate the wall heat flux from the known free-stream parameters, wall temperature and skin-friction coefficient. The results are presented in Table 1 and yield values of Q_+ that are very close to those obtained by DNS (Zhang et al., 2018). Moreover, as can be seen from Table 1, good agreement is achieved despite the rather large free-stream Mach numbers.

SKIN-FRICTION LAW

The skin-friction law under any wall-heat-transfer conditions has the form (Vigdorovich, 2025)

$$\ln Re_u = \frac{\kappa(\phi_\infty - \phi_w)}{\tan\vartheta\sqrt{\tfrac{1}{2}C_f}} + \kappa[Q_1(\phi_\infty, \phi_w) - D_1(Pr, n, Q_+)]$$

r	$2St/C_f$	Q_+	$Q_+(DNS)$	M_∞	Re_τ
0.899	1.164	-0.1375	-0.14	5.84	450
0.887	1.194	-0.0198	-0.02	5.86	453
0.888	1.184	-0.0606	-0.06	7.87	480

Table 1. Heat-flux values calculated with the help of formulas for the recovery and Reynolds-analogy factors (26) and (27) and the DNS data by Zhang et al. (2018).

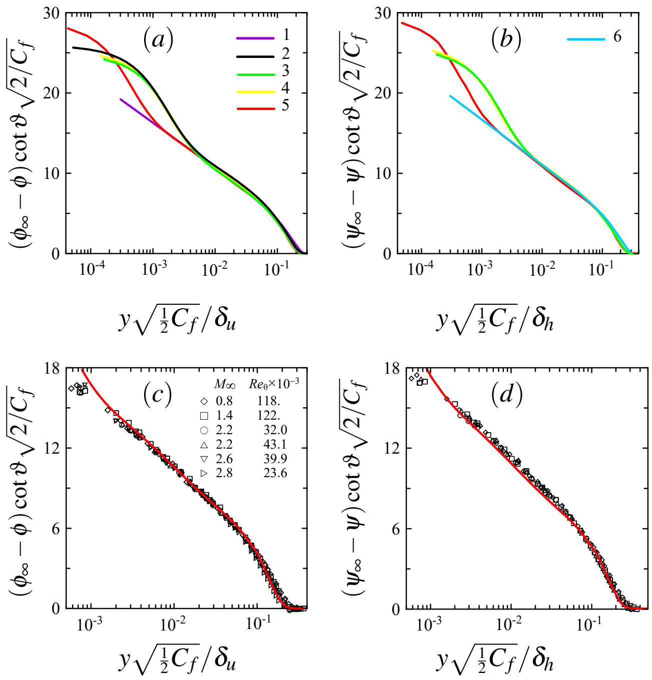

Figure 4. Calculated and experimental velocity and temperature profiles in supersonic turbulent boundary layers on an adiabatic plate plotted in similarity variables (24) and (25).

$$+A_0 + \frac{1}{2}\ln\frac{h_w}{h_\infty} + O\left(\sqrt{C_f}\right), \quad Re_u = \frac{\rho_\infty u_\infty \delta_u}{\mu_w}$$

and contains one empirical function $D_1(Pr, n, Q_+)$. Here, we use the Reynolds number Re_u formed with the velocity-defect thickness δ_u. In the particular case of an adiabatic plate, it can be written as

$$\sqrt{\frac{C_f}{2}} = \kappa\vartheta\cot\vartheta[\ln Re_u + (1-\kappa A_3)\ln\cos\vartheta - A_0\cos^2\vartheta$$

$$+(\kappa A_2 - E_0)\sin^2\vartheta + \kappa C]^{-1}. \quad (28)$$

In figure 5 formula (28) is compared with a large number of experimental data collected by Fernholz & Finley (1977); Fernholz et al. (1981). The experimental points in figure 5 are obtained in a very wide range of Reynolds numbers at $M_\infty \leq 5$.

In figure 6, the skin-friction law obtained by Vigdorovich (2025) for non-zero wall heat flux is compared with available experimental and DNS data for the boundary layer on a cooled and heated plate.

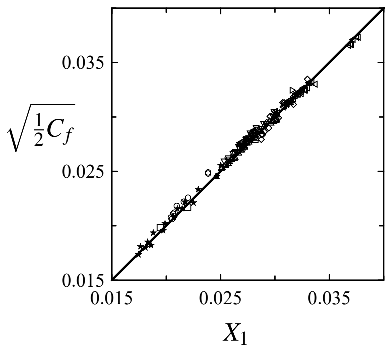

Figure 5. Skin-friction law for the compressible turbulent boundary layer on an adiabatic plate. The bisector of the right angle corresponds to formula (28), while X_1 is the right-hand side of equality (28).

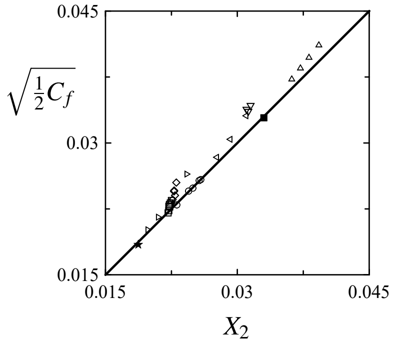

Figure 6. Skin-friction law for supersonic turbulent boundary layers on a plate with heat transfer. The bisector of the right angle corresponds to the theoretical formula.

CONCLUDING REMARKS

We develop a rational asymptotic theory of the compressible turbulent boundary layer on a flat plate, whose first main element are closure relations connecting the Reynolds-tensor components and turbulent enthalpy flux with the mean velocity and enthalpy gradients. Together with the boundary layer and energy equations, they give a well-posed boundary-value problem for the mean velocity and enthalpy fields (Vigdorovich, 2023a). Derived from first principles, these closure relations are not based on any partial hypotheses about the nature of turbulent exchange or turbulence models and therefore allow us to describe the flow under consideration at a new higher level of rigor.

The second important element of the theory is its asymptotic character. When describing the flow in the near-wall region, we introduce a small parameter of the problem ε, which is proportional to the Mach number formed with the friction velocity and the speed of sound at the wall, and construct the solution in two characteristic regions of the boundary layer — viscous and logarithmic — by the method of matched asymptotic expansions in this small parameter (Vigdorovich, 2023b, 2024).

For an asymptotic description of the flow in the outer region, a special change of variables in the boundary-layer and energy equations is proposed, which makes it possible to construct the solution in the form of asymptotic expansions at large values of the logarithm of the Reynolds number based on the boundary-layer thickness. Together with the results known for an incompressible fluid (Vigdorovich, 1993, 2017), this, in particular, shows that an adequate small parameter for near-wall turbulent flows is the reciprocal of the logarithm of Reynolds number.

ACKNOWLEDGMENT

The author would like to thank S. Pirozzoli and M. Bernardini, who kindly provided their DNS data.

The work was completed under the State Assignement for Lomonosov Moscow State University.

REFERENCES

Appelbaum, J., Gibis, T., Pirozzoli, S. & Wenzel, C. 2025 The onset of outer-layer self-similarity in turbulent boundary layers. *J. Fluid Mech.* **1015**, A37.

Fernholz, H. H. & Finley, P. J. 1977 A critical compilation of compressible turbulent boundary layer data. *AGARDograph* No. 223, 480 p.

Fernholz, H. H., Finley, P. J. & Mikulla, V. 1981 A further compilation of compressible boundary layer data with a survey of turbulence data. *AGARDograph* No. 263, 222 p.

Pirozzoli, S. & Bernardini, M. 2011 Turbulence in supersonic boundary layers at moderate Reynolds number. *J. Fluid Mech.* **668**, 120–168.

Pirozzoli, S. & Bernardini, M. 2013 Probing high-Reynolds-number effects in numerical boundary layers. *Phys. Fluids* **25**, 021704.

Schlatter, P. & Örlü, R. 2010. Assessment of direct numerical simulation data of turbulent boundary layers. *J. Fluid Mech.* **659**, 116–126.

Van Driest, E. R. 1951 Turbulent boundary layer in compressible fluids. *J. Aeronaut. Sci.* **18**, 145–160.

Van Driest, E. R. 1956 The problem of aerodynamic heating. *Aeronaut. Engng. Rev.* **15**, 26–41.

Vigdorovich, I. I. 1993 Asymptotic analysis of turbulent boundary layer flow on a flat plate at high Reynolds numbers. *Fluid Dynamics* **28** (4), 514–523.

Vigdorovich, I. I. 2003 Similarity laws for the velocity and temperature profiles in the wall region of a turbulent boundary layer with injection and suction. *Doklady Phys.* **48**(9), 528–532.

Vigdorovich, I. I. 2017 Turbulent thermal boundary layer on a plate. Reynolds analogy and heat transfer law over the entire range of Prandtl numbers. *Fluid Dynamics* **52** (5), 631–645.

Vigdorovich, I. 2023 Supersonic turbulent boundary layer on a plate. I. Closure relations. *Phys. Fluids* **35** (11), 115122.

Vigdorovich, I. 2023 Supersonic turbulent boundary layer on a plate. II. Flow in the wall region and the Crocco integral. *Phys. Fluids* **35** (11), 115123.

Vigdorovich, I. 2024 Supersonic turbulent boundary layer on a plate. III. Laws of the wall for velocity and temperature. *Phys. Fluids* **36** (8), 085179.

Vigdorovich, I. 2025 Supersonic turbulent boundary layer on a plate. Universal velocity and temperature defect laws and skin-friction law at moderate free-stream Mach numbers. *J. Fluid Mech.* 1020, A17.

Walz, A. 1966 *Strömungs- und Temperaturgrenzschichten.* Braun Verlag, Karlsruhe.

Zhang, C., Duan, L. & Choudhari, M. M. 2018 Direct numerical simulation database for supersonic and hypersonic turbulent boundary layers. *AIAA J.* **56** (11), 4297–4311.